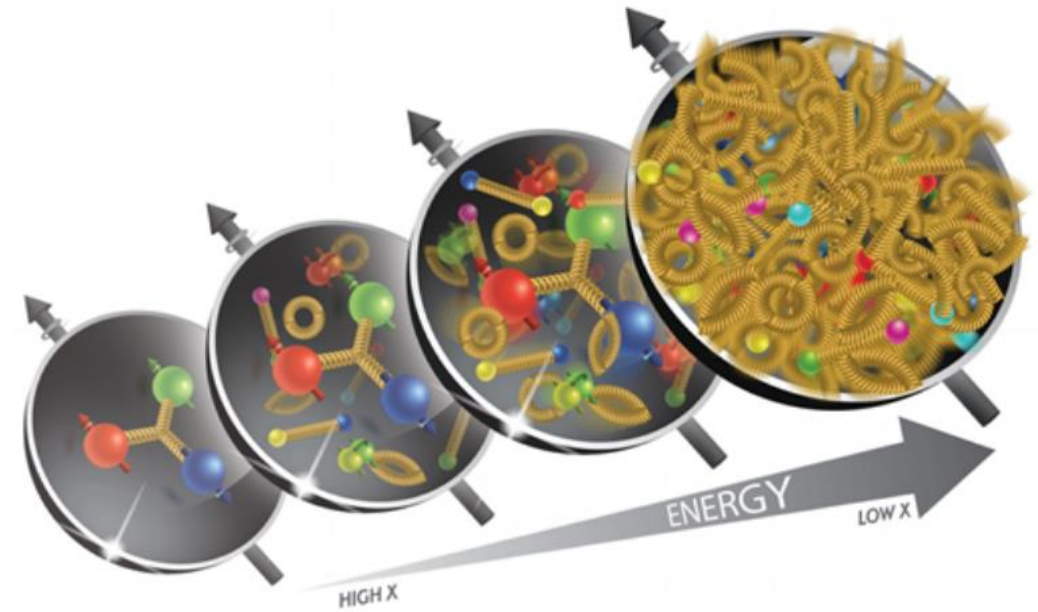
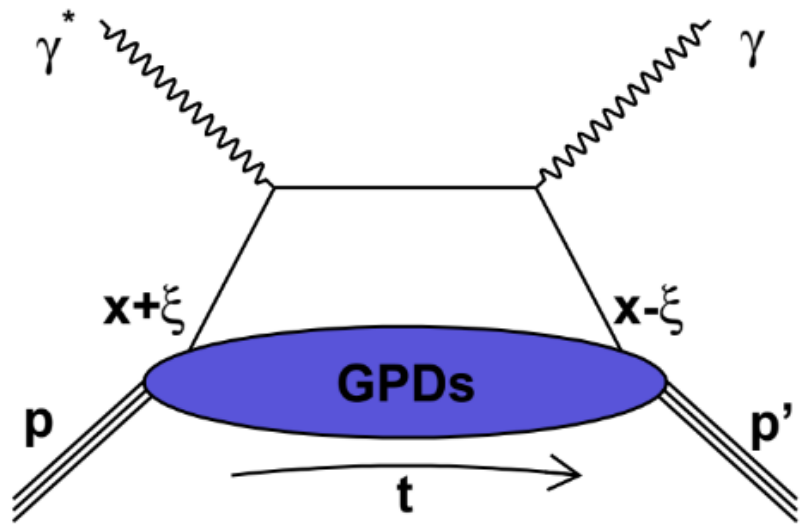


Deeply Virtual Compton Scattering and Spatial Imaging



Carlos Muñoz Camacho
IJCLab-Orsay (CNRS/IN2P3, France)

Outline

□ Lecture 1: Introduction

- Elastic scattering, form factors (FFs)
- Deep Inelastic scattering, parton distribution functions (PDFs)
- Exclusive reactions, Generalized Parton Distributions (GPDs)

□ Lecture 2: Deeply Virtual Compton Scattering

- Experimental results on proton targets
- Flavor separation using quasi-free neutrons

□ Lecture 3: Deeply Virtual Meson Production

- Rosenbluth separation
- Access to transversity GPDs
- Flavor decomposition

□ Lecture 4: Models and outlook

- GPD models and parametrizations
- 12 GeV experimental program on GPDs

□ Lecture 5: Electron-Ion Collider

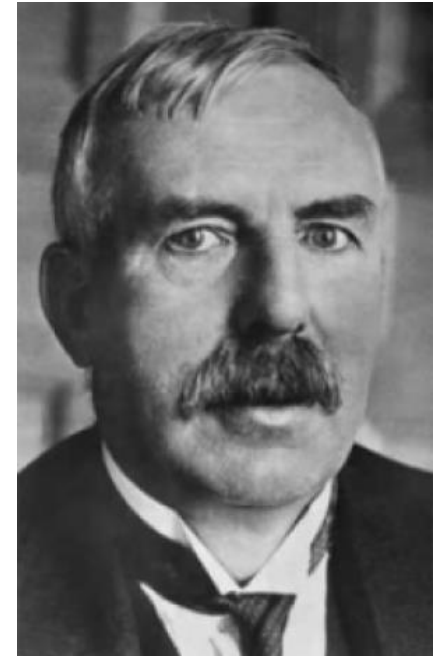
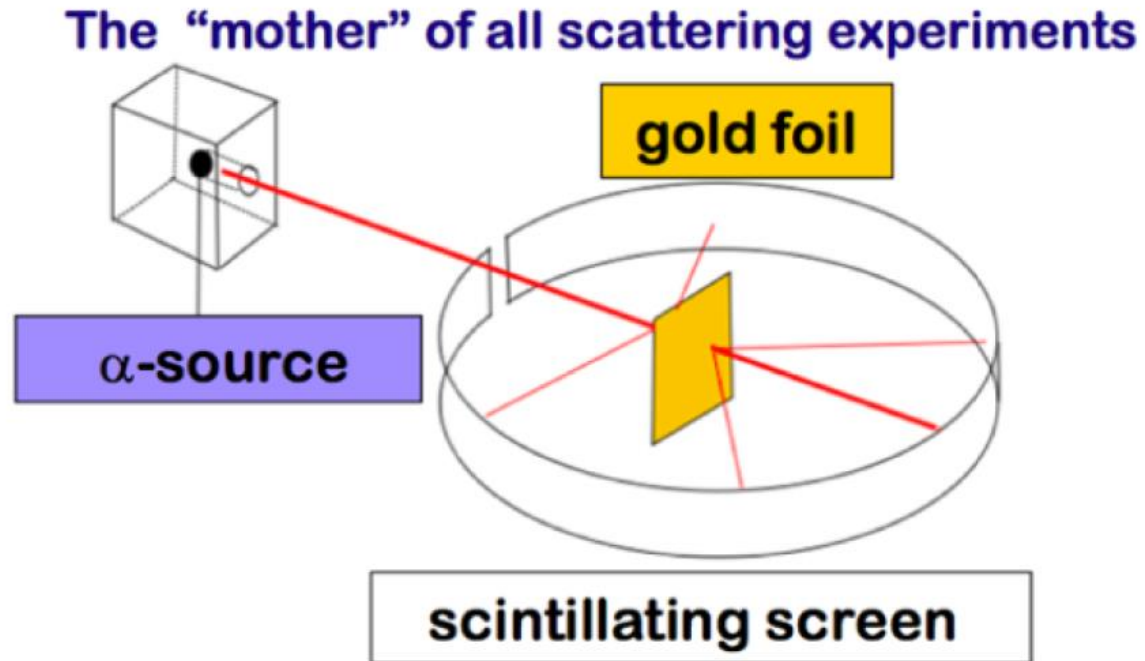
- Imaging gluons inside the nucleon
- The EIC project

Lecture 1

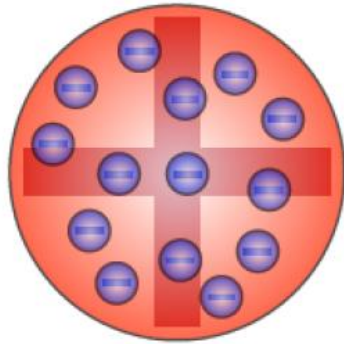
- Introduction to scattering experiments
- Elastic scattering and form factors of the nucleon
- Deep Inelastic Scattering and parton distribution functions (PDFs)
 - Factorization at high Q^2
- Off-forward Compton Scattering
 - Generalized Parton Distributions (GPDs)
 - Deeply Virtual Compton Scattering (DVCS)
 - Interference with Bethe-Heitler (BH) process

Introduction

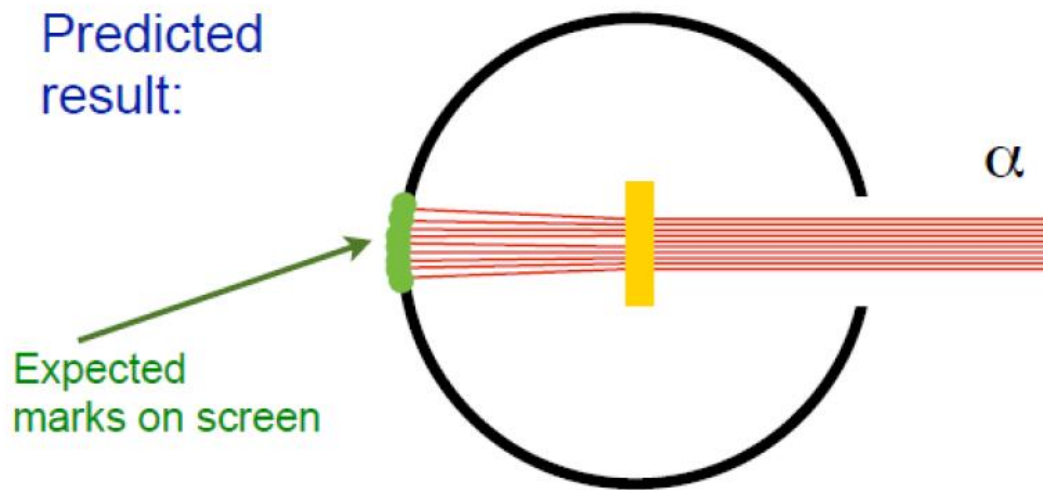
The first exploration of subatomic structure was undertaken by Rutherford in Manchester using gold atoms as target and α particles as probes



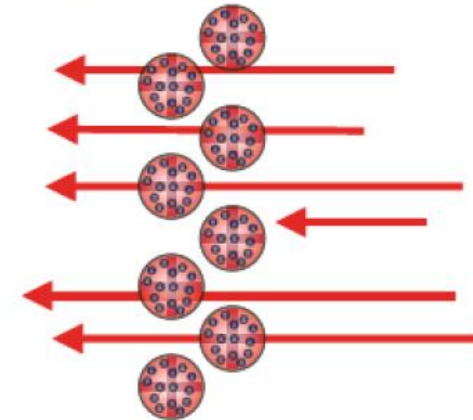
Rutherford experiment: expectation



Thomson's
Plum Pudding Model

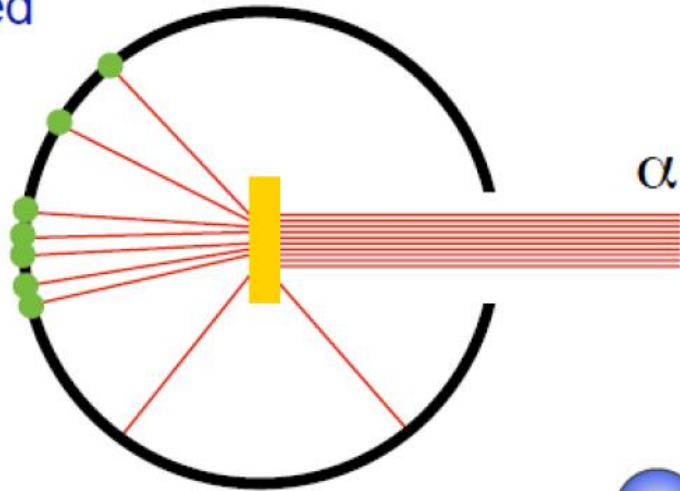


Detail of gold foil (Thomson):

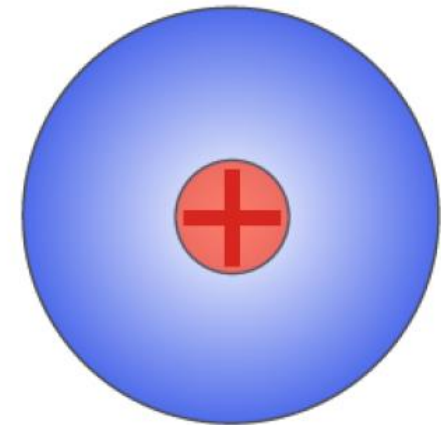
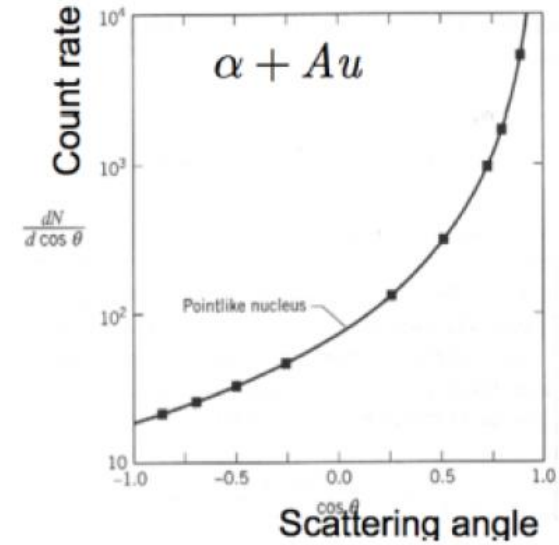
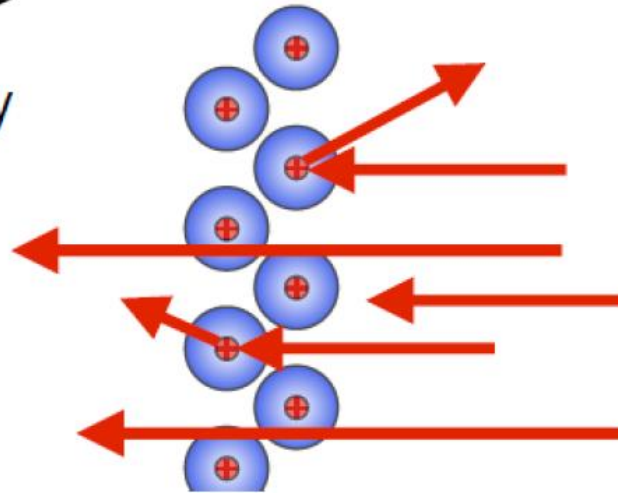


Rutherford experiment: result

Observed result:



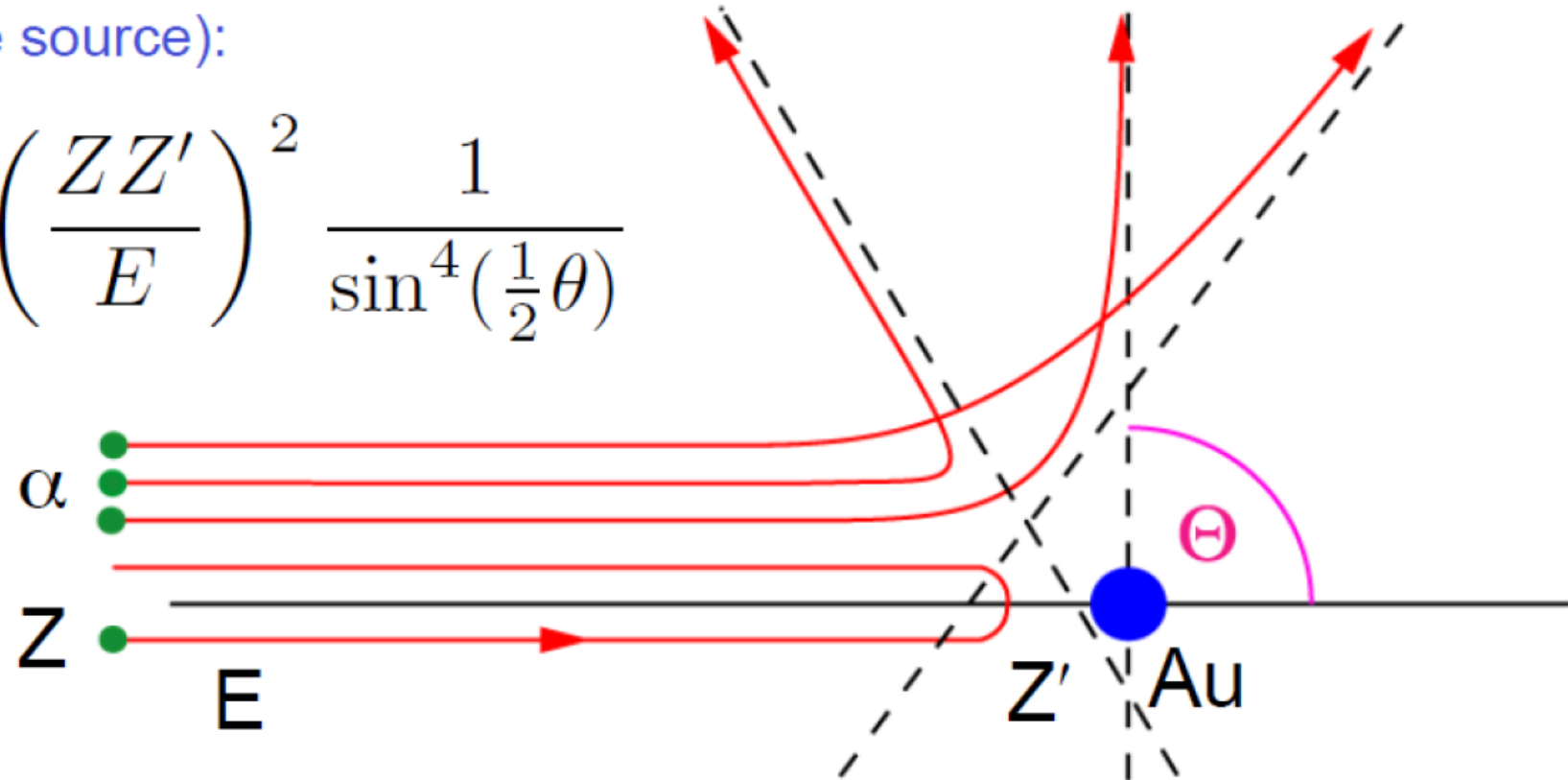
Positive Nucleus Theory explain α deflection:



Rutherford experiment: result

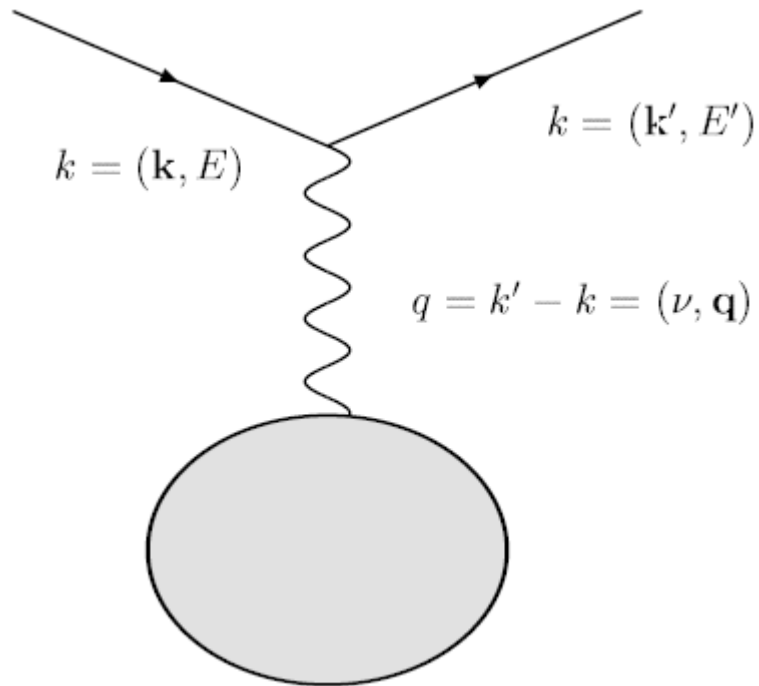
Elastic scattering of charged particles in Coulomb field (point-like source):

$$\frac{d\sigma}{d\Omega} = \left(\frac{ZZ'}{E} \right)^2 \frac{1}{\sin^4\left(\frac{1}{2}\theta\right)}$$



Probing the structure of the proton: elastic scattering

$ep \rightarrow ep$



Probing internal structure
through electron scattering

$$\frac{d\sigma}{d\Omega} = \left(\frac{d\sigma}{d\Omega} \right)_{\text{point}} |F(\mathbf{q})|^2$$

Form factor

For a spinless target with charge distribution $\rho(\mathbf{x})$

$$F(\mathbf{q}) = \int \rho(\mathbf{x}) e^{i\mathbf{q}\cdot\mathbf{x}} d^3x$$

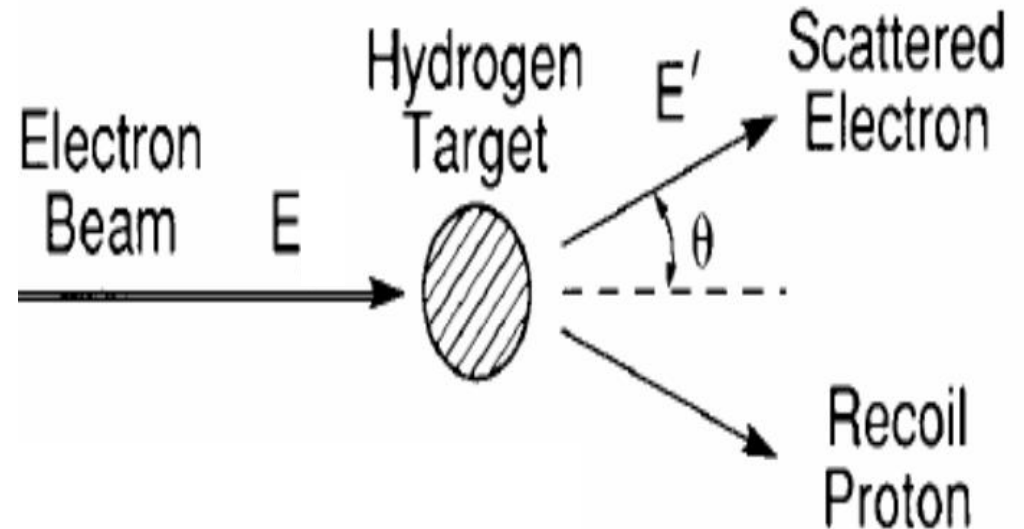
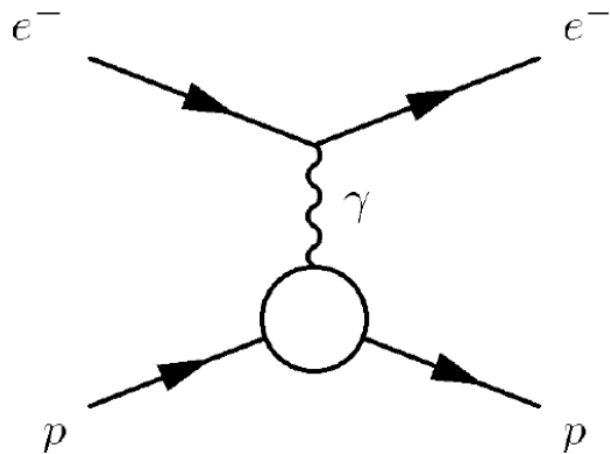
Elastic scattering: spin $\frac{1}{2}$ particle

Rosenbluth (1950):

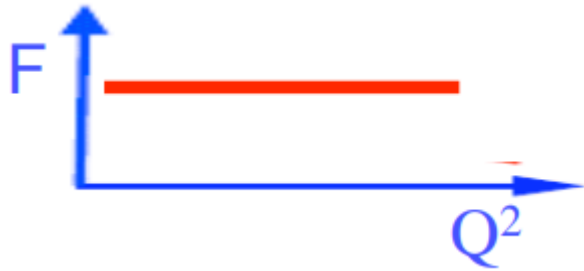
$$\frac{d\sigma}{d\Omega}(E) = \sigma_M(E) \left(\frac{E'}{E}\right) \left(\frac{G_{Ep}^2(q^2) + \tau G_{Mp}^2(q^2)}{1 + \tau} + 2\tau G_{Mp}^2(q^2) \tan^2 \frac{\theta}{2} \right)$$

Point-like
Mott cross section

$$\tau = \frac{-q^2}{4M^2}$$

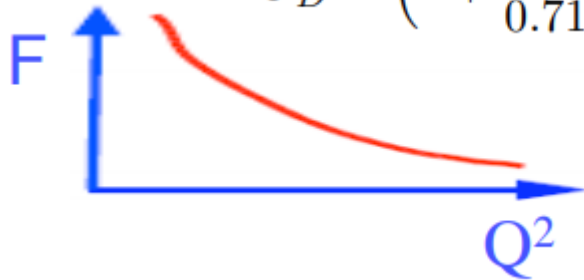


Charge density inside protons and neutrons



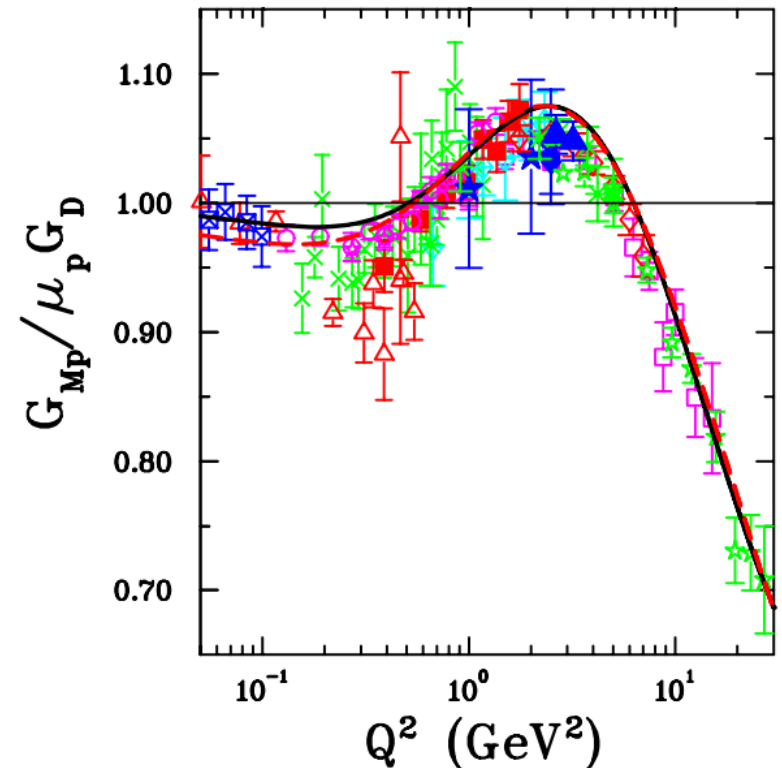
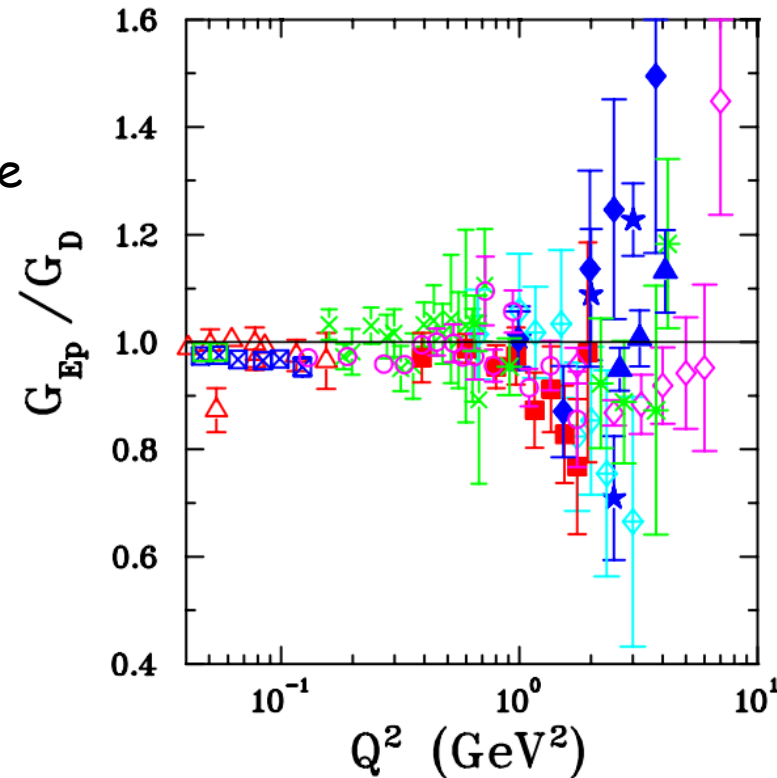
Point-charge: $F(Q^2)=\text{constant}$
photon always sees all of its charge

$$G_D = \left(1 + \frac{Q^2}{0.71}\right)^{-2}$$



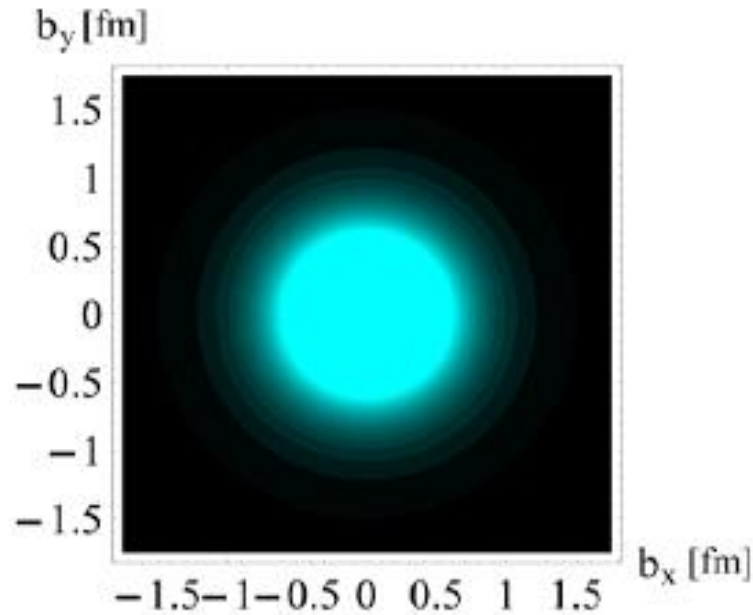
Elastic electron-proton scattering:
photon sees less charge as Q^2 increases

Experimental data as a function of the momentum transfer $Q^2=-q^2$:

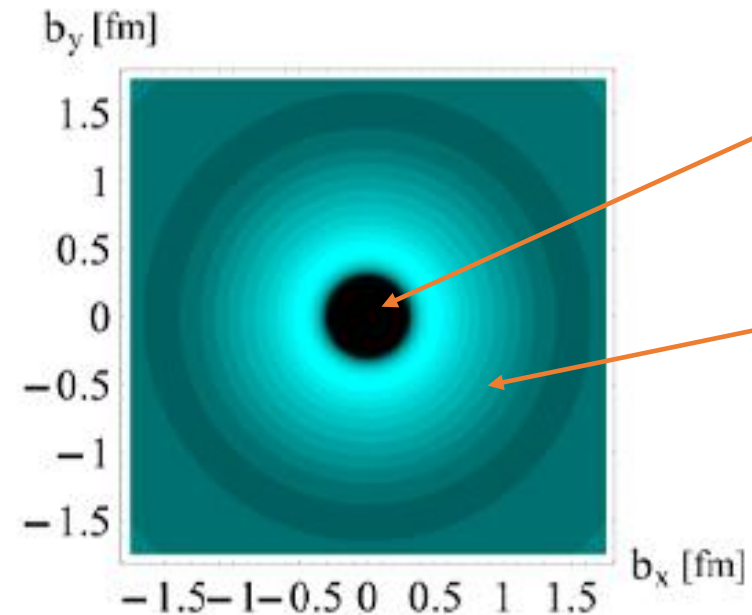


Punjabi et al. (2015)

Charge density inside protons and neutrons



Proton

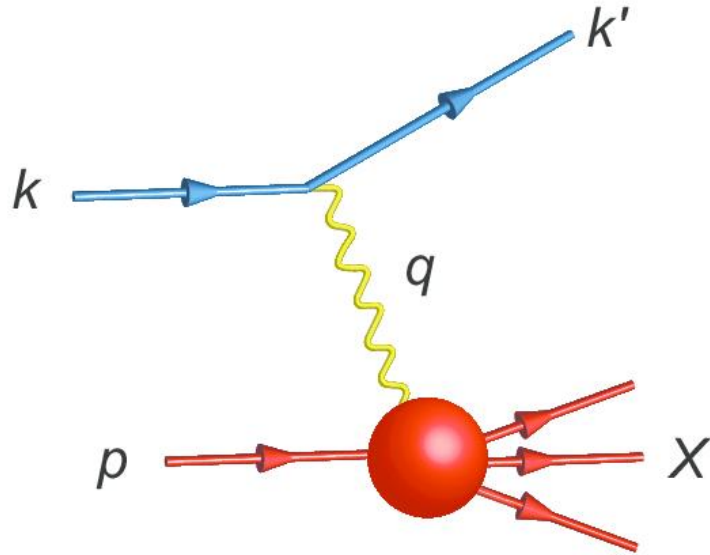


Negative inner core

Positive outer surface

Neutron

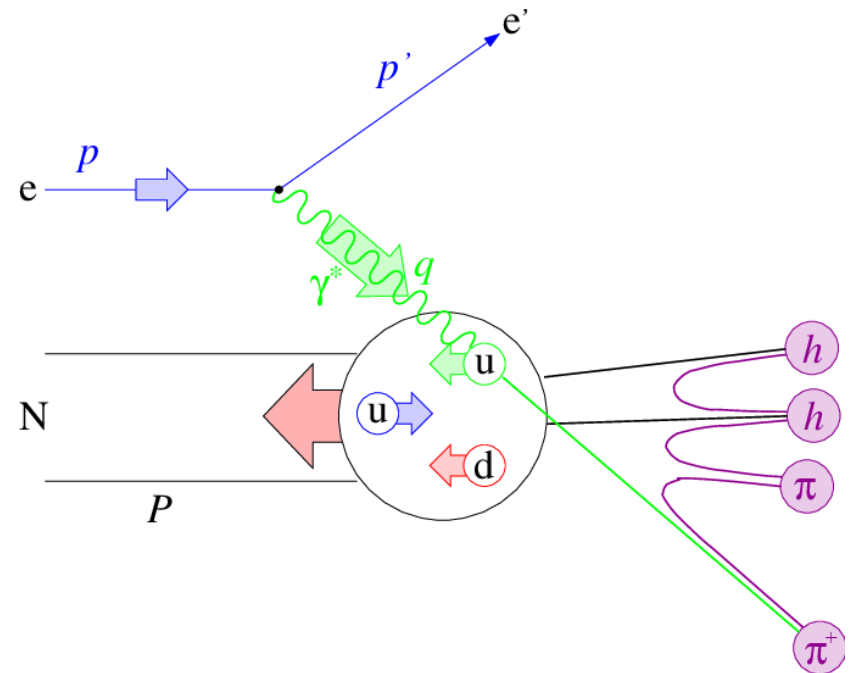
Deep inelastic scattering



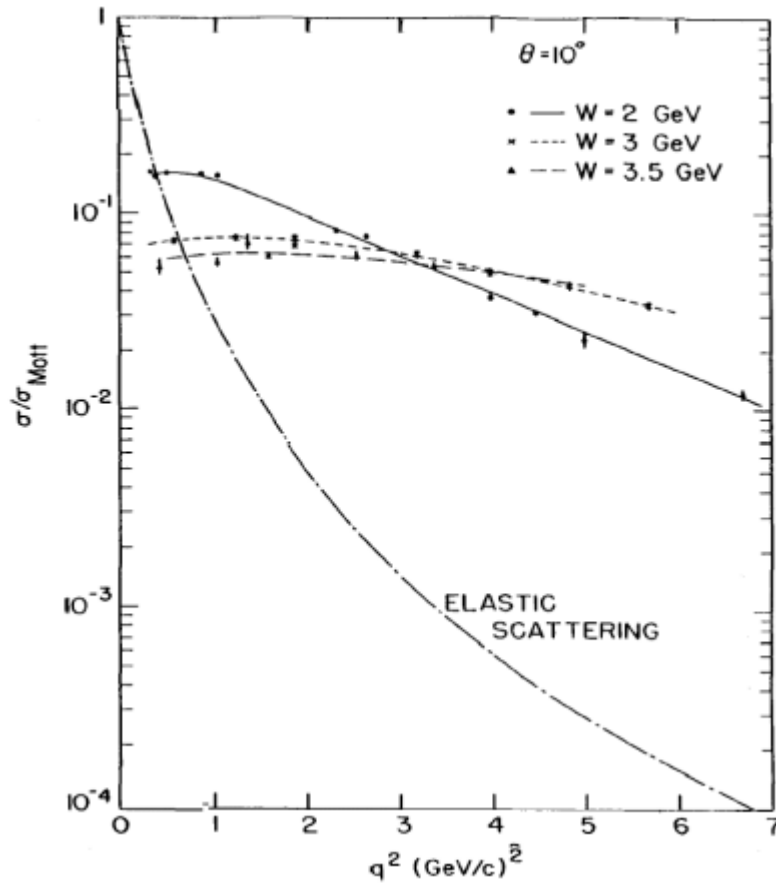
Invariant mass of the hadronic state:

$$W^2 = (2M\nu + M^2 - Q^2) \quad \nu = E - E'$$

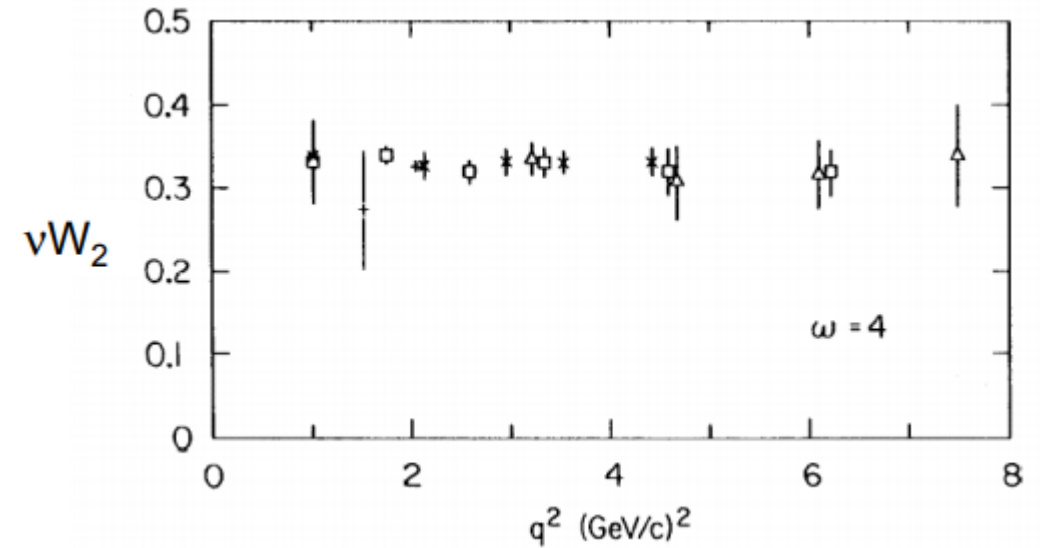
$$\frac{d^2\sigma}{d\Omega dE'}(E, E', \theta) = \sigma_M \left(W_2(\nu, q^2) + 2W_1(\nu, q^2) \tan^2 \frac{\theta}{2} \right)$$



Unexpected results from SLAC e-P scattering



$$\frac{d\sigma}{d\Omega} = \frac{d\sigma}{d\Omega_{point}} |F(q)|^2$$



- The ratio σ/σ_{Mott} : no Q^2 dependence
- Structure function W_2 has no Q^2 dependence

Scattering against a point-like particle

$$2MW_1(\nu, q^2) = F_1(\omega)$$

$$\nu W_2(\nu, q^2) = F_2(\omega)$$

Bjorken Scaling

Parton model

Feynman (1969)

- Proton composed of point-like partons, from which the electrons scattered incoherently
- In an infinite momentum frame of reference: time dilation slowed down the motion of constituents
- Partons are assumed not to interact with one another while the virtual photon is exchanged (impulse approximation)

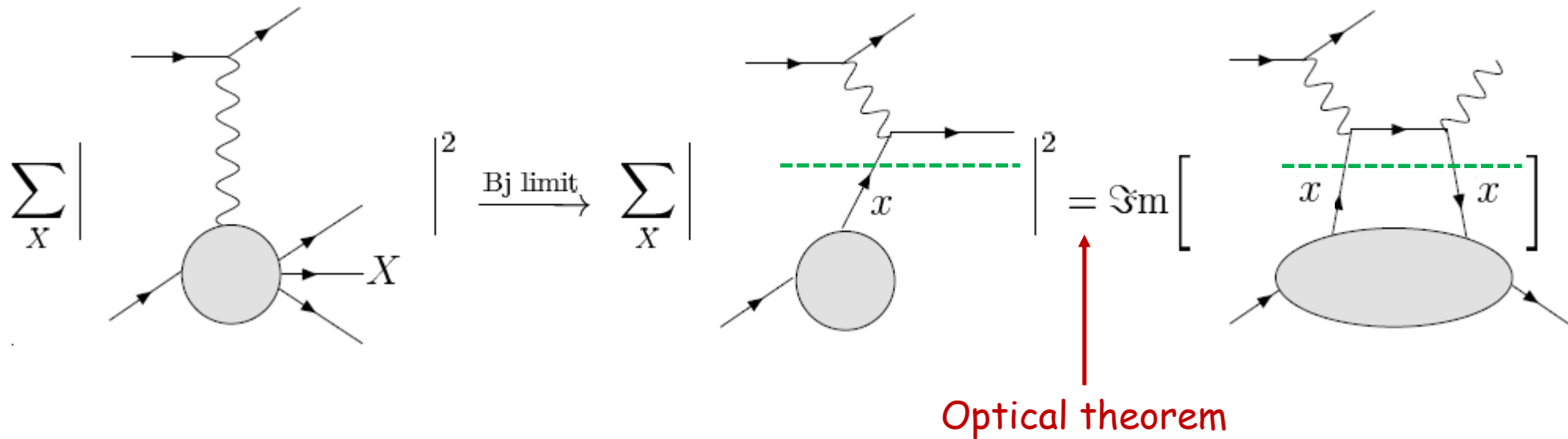
In this theory, electrons scatter from constituents that are "free" and the scattering reflects the properties and motion of the constituents

The assumption of near-vanishing parton-parton interaction during electron scattering (at high Q^2) was later shown to be a consequence of QCD known as *asymptotic freedom*

Factorization

$$\sigma_{\text{DIS}}(x, Q^2) = \sum_i q_i(x) \sigma_{eq \rightarrow eq}(x, Q^2)$$

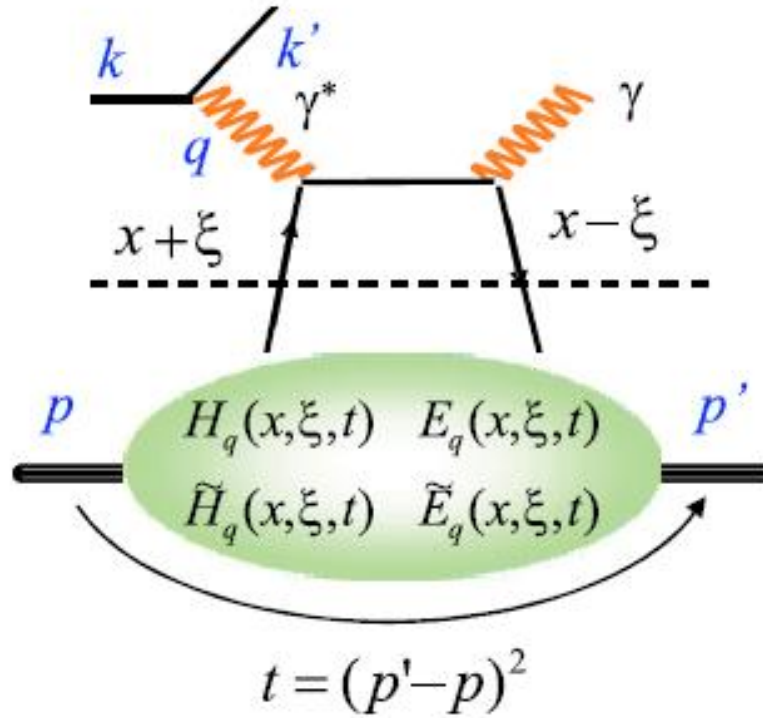
Parton Distribution Function (PDF)



$$x = \frac{Q^2}{2P \cdot q} = x_B$$

Off-forward Compton scattering

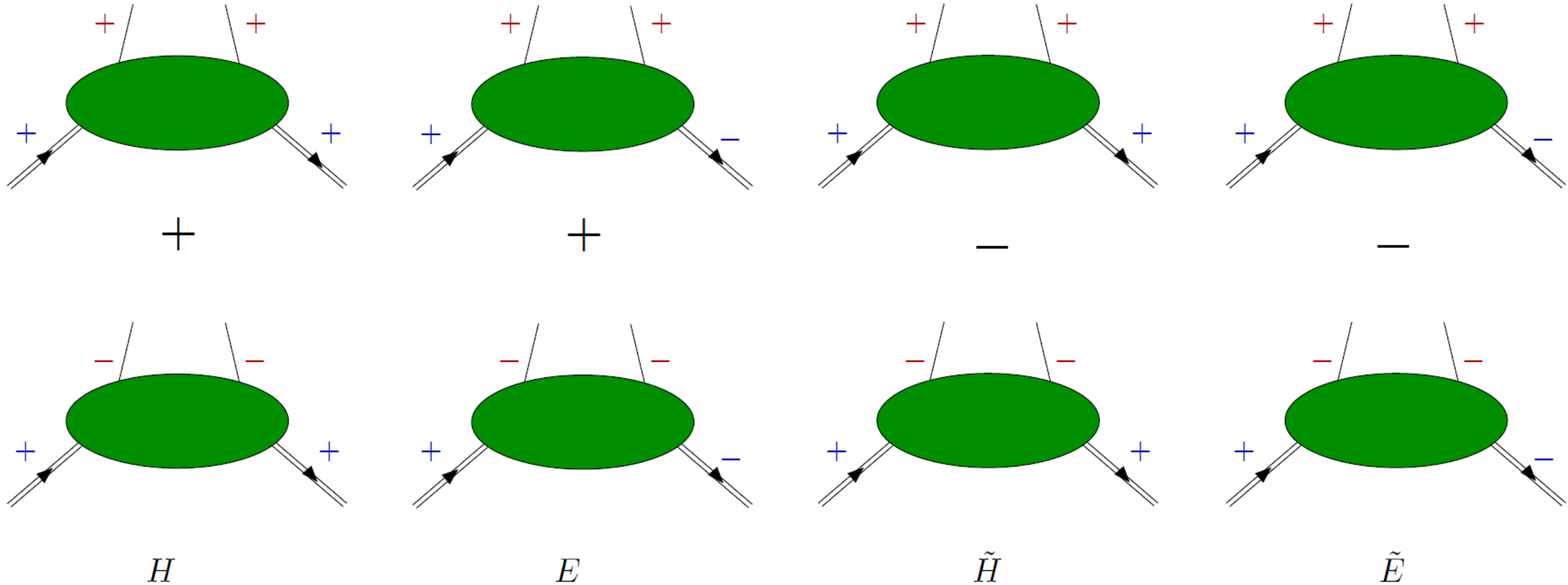
$$e p \rightarrow e' p' \gamma$$



$$\gamma^* p \rightarrow p' \gamma$$

Deeply Virtual Compton Scattering (DVCS)

Generalized Parton Distribution (GPDs)



Properties of GPDs

Forward limit:

$$\begin{aligned} H^f(x, 0, 0) &= q_f(x), \\ \tilde{H}^f(x, 0, 0) &= \Delta q_f(x) \end{aligned}$$

Polynomiality:

$$\int_{-1}^1 dx x^n H(x, \xi, t) = a_0 + a_2 \xi^2 + a_4 \xi^4 + \dots + a_n \xi^n$$

1st moments:

$$\int_{-1}^1 dx H^f(x, \xi, t) = F_1^f(t) \quad \forall \xi$$

$$\int_{-1}^1 dx E^f(x, \xi, t) = F_2^f(t) \quad \forall \xi$$

$$\int_{-1}^1 dx \tilde{H}^f(x, \xi, t) = G_A^f(t) \quad \forall \xi$$

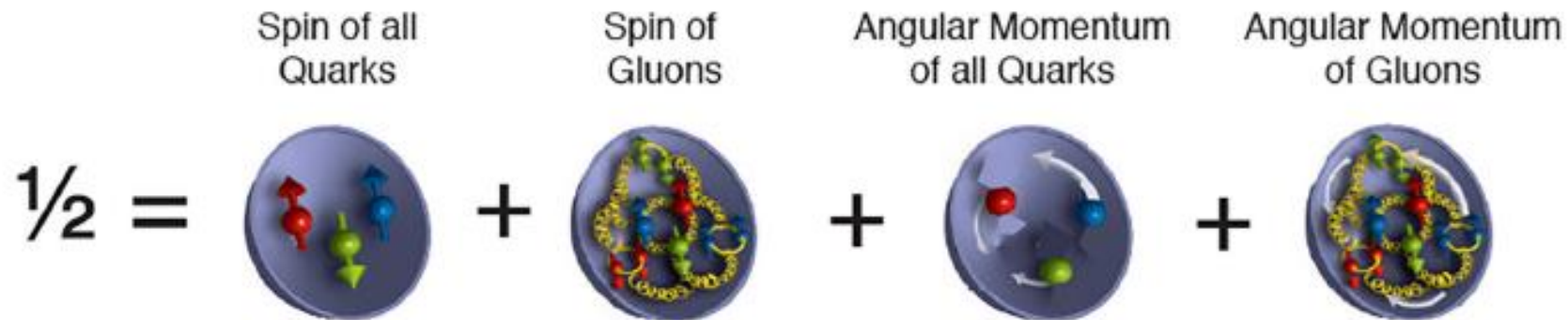
$$\int_{-1}^1 dx \tilde{E}^f(x, \xi, t) = G_p^f(t) \quad \forall \xi$$

Ji's sum rule

X. Ji (1996)

Second moment of GPDs H+E:

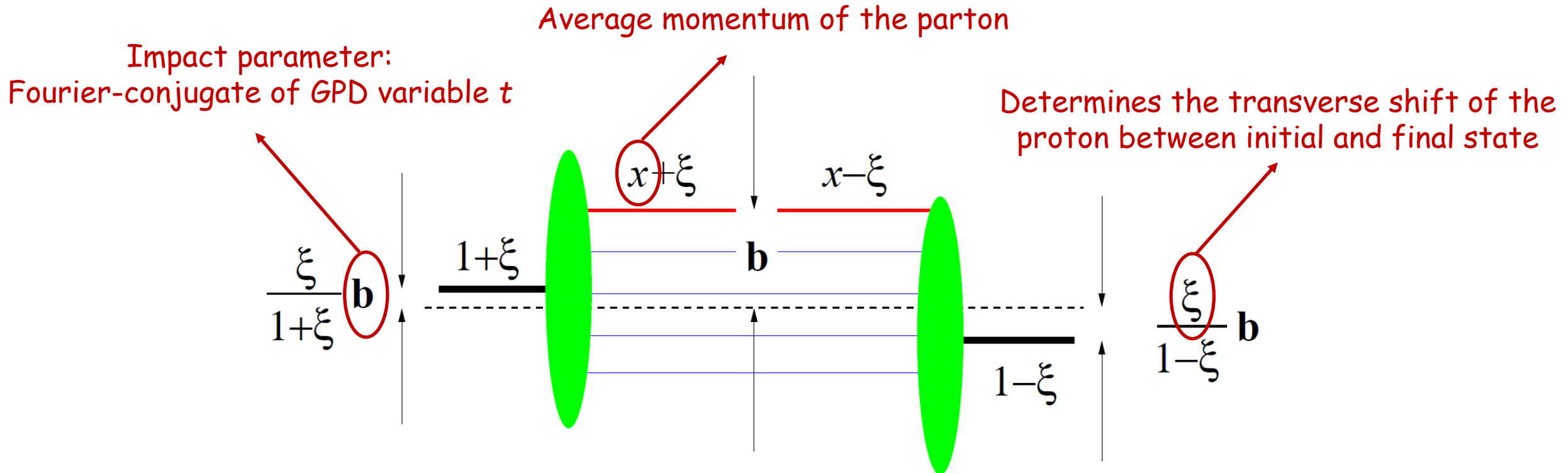
$$\frac{1}{2} \int_{-1}^1 dx x [H^f(x, \xi, 0) + E^f(x, \xi, 0)] = J^f \quad \forall \xi$$



$$\frac{1}{2} = \underbrace{\frac{1}{2} \Delta \Sigma + L_q}_{J_q} + J_g$$

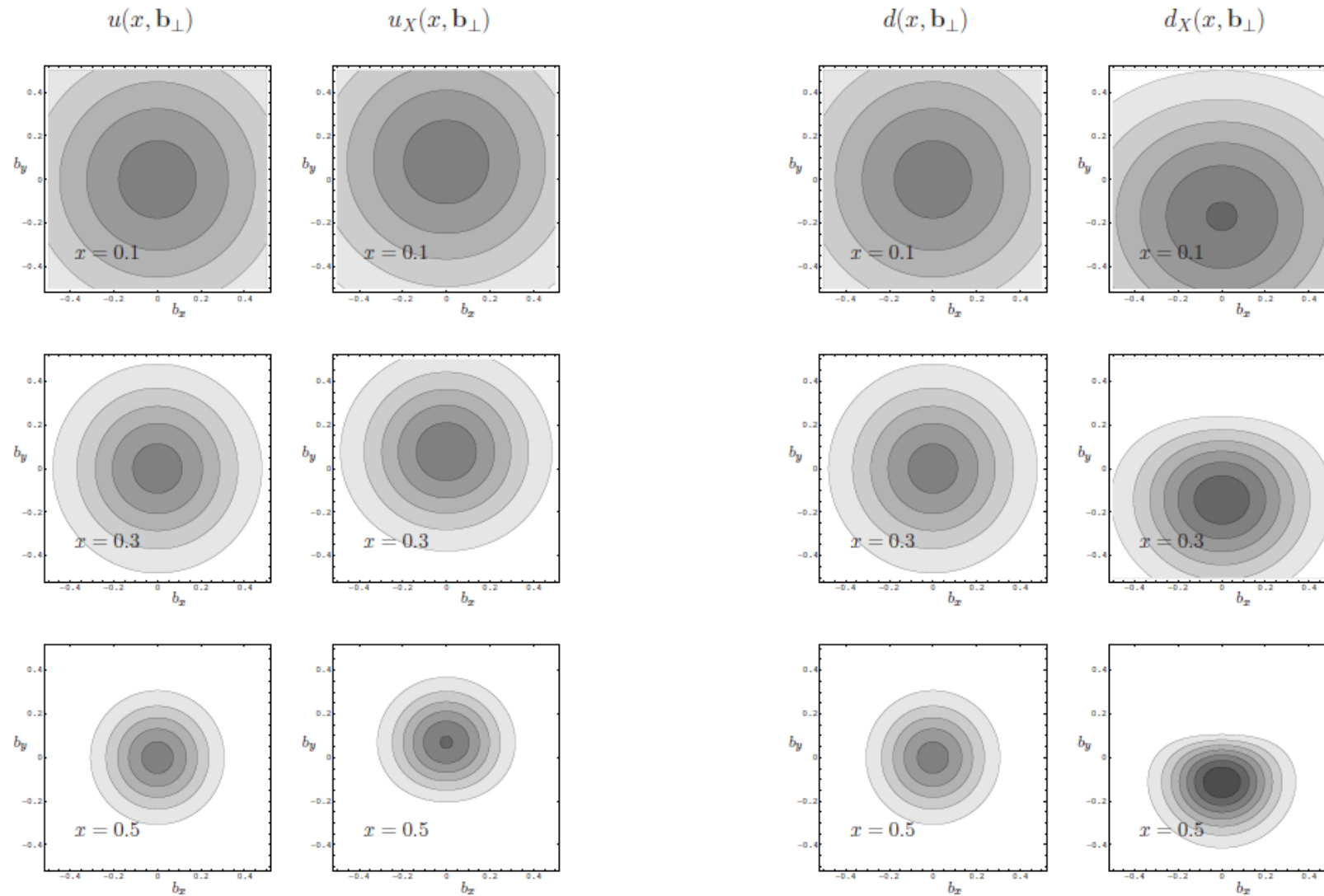
Physical interpretation of GPDs

Burkardt (2000), Diehl (2002)

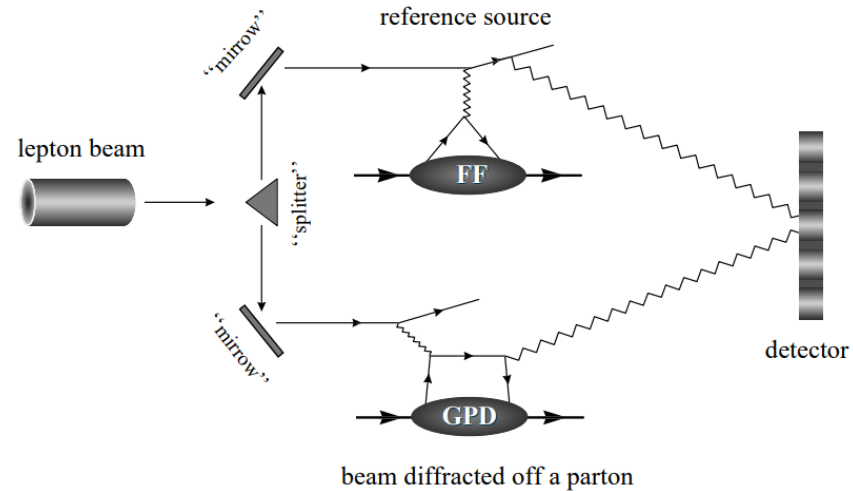
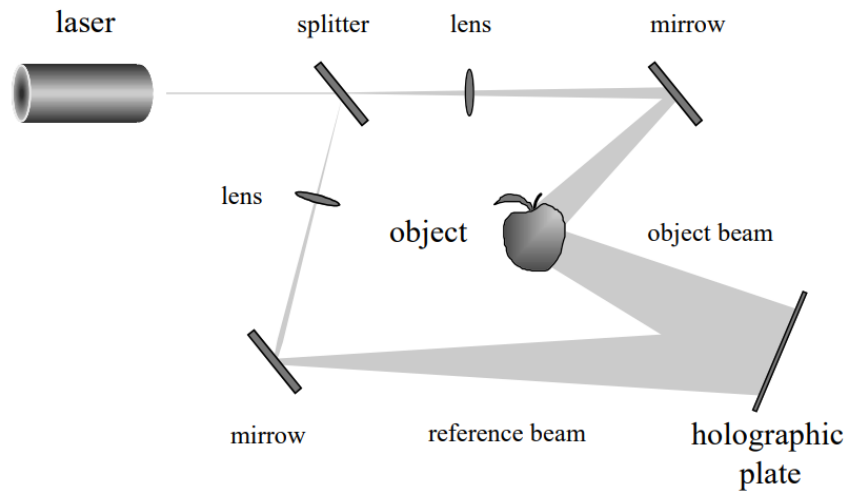
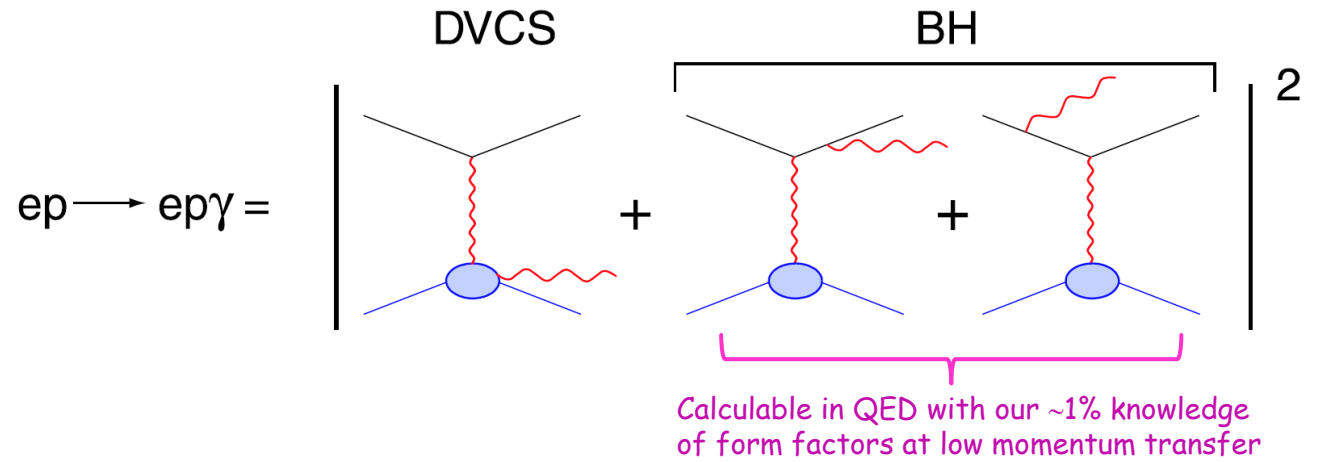
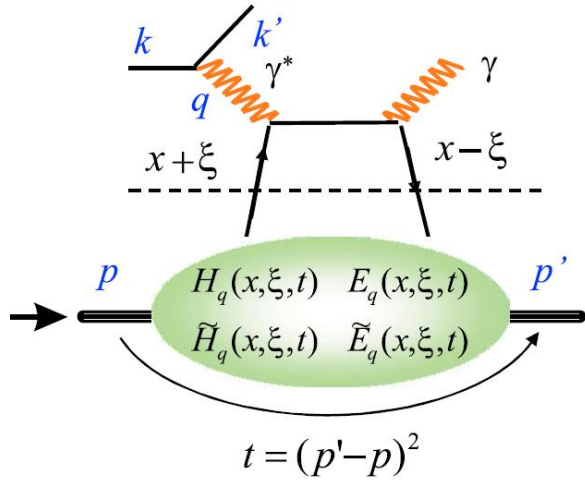


Transverse position of partons and longitudinal momentum

3D imaging of the proton with DVCS



DVCS and Bethe-Heitler



DVCS and BH interference

$$|\mathcal{T}(\pm ep \rightarrow \pm ep\gamma)|^2 = |\mathcal{T}^{BH}|^2 + |\mathcal{T}^{DVCS}|^2 \mp \mathcal{I}$$

When only 1 quark of the proton is involved in the reaction:

$$\begin{aligned} d^5 \vec{\sigma} - d^5 \overleftarrow{\sigma} &= \Im(T^{BH} \cdot T^{DVCS}) \\ d^5 \vec{\sigma} + d^5 \overleftarrow{\sigma} &= |BH|^2 + \Re(T^{BH} \cdot T^{DVCS}) + |DVCS|^2 \end{aligned}$$

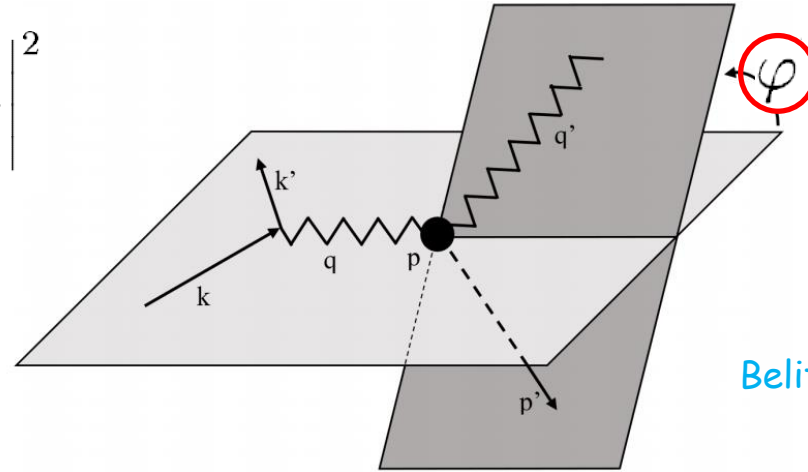
Using a polarized electron beam

$$\sigma(ep \rightarrow ep\gamma) = \underbrace{|BH|^2}_{\text{Known to } \sim 1\%} + \underbrace{\mathcal{I}(BH \cdot DVCS)}_{\text{Linear combination of GPDs}} + \underbrace{|DVCS|^2}_{\text{Bilinear combination of GPDs}}$$

Azimuthal dependence of the DVCS cross section

$$\frac{d^5\sigma}{dQ^2 dx_B d\varphi_e dt d\varphi} = \frac{\alpha^3 x_B y}{16\pi^2 Q^2 \sqrt{1 + 4x_B^2 M^2/Q^2}} \left| \frac{\mathcal{T}}{e^3} \right|^2$$

$$|\mathcal{T}|^2 = |\mathcal{T}_{\text{BH}}|^2 + |\mathcal{T}_{\text{DVCS}}|^2 + \mathcal{I}$$



Belitsky, Müller, Kirchner (2000)

$$|\mathcal{T}_{\text{BH}}|^2 = \frac{e^6}{x_B^2 y^2 [1 + 4x_B^2 M^2/Q^2]^2 t \mathcal{P}_1(\varphi) \mathcal{P}_2(\varphi)} \left\{ c_0^{\text{BH}} + \sum_{n=1}^2 c_n^{\text{BH}} \cos(n\varphi) + s_1^{\text{BH}} \sin \varphi \right\},$$

$$|\mathcal{T}_{\text{DVCS}}|^2 = \frac{e^6}{y^2 Q^2} \left\{ c_0^{\text{DVCS}} + \sum_{n=1}^2 [c_n^{\text{DVCS}} \cos(n\varphi) + s_n^{\text{DVCS}} \sin(n\varphi)] \right\},$$

$$\mathcal{I} = \frac{\pm e^6}{x_B y^3 t \mathcal{P}_1(\varphi) \mathcal{P}_2(\varphi)} \left\{ c_0^{\mathcal{I}} + \sum_{n=1}^3 [c_n^{\mathcal{I}} \cos(n\varphi) + s_n^{\mathcal{I}} \sin(n\varphi)] \right\},$$

GPDs and Compton Form Factors (CFFs)

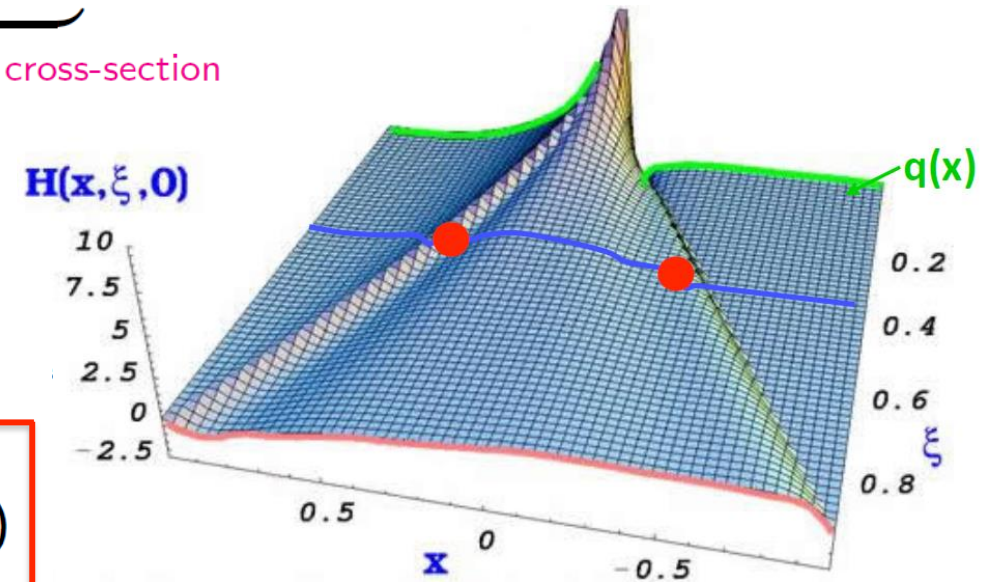
$$\mathcal{T}^{DVCS} = \int_{-1}^{+1} dx \frac{H(x, \xi, t)}{x - \xi + i\epsilon} + \dots =$$

$$\underbrace{\mathcal{P} \int_{-1}^{+1} dx \frac{H(x, \xi, t)}{x - \xi}}_{\text{Access in helicity-independent cross section}} - \underbrace{i\pi H(x = \xi, \xi, t)}_{\text{Access in helicity-dependent cross-section}} + \dots$$

Access in helicity-independent cross section

Access in helicity-dependent cross-section

$$\begin{array}{l} \text{CFF} \\ \downarrow \\ \mathcal{H} = \int_{-1}^{+1} dx \frac{H(x, \xi, t)}{x - \xi + i\epsilon} = \underbrace{\mathcal{P} \int_{-1}^{+1} dx \frac{H(x, \xi, t)}{x - \xi}}_{\text{GPD}} - \underbrace{i\pi H(x = \xi, \xi, t)} \end{array}$$



Accessing GDPs from DVCS

Polarized beam, unpolarized target (BSA)

$$d\sigma_{LU} = \sin \phi \cdot \mathcal{I}m\{F_1 \mathcal{H} + x_B(F_1 + F_2)\tilde{\mathcal{H}} - kF_2 \mathcal{E}\}d\phi$$

Unpolarized beam, longitudinal target (ITSA)

$$d\sigma_{UL} = \sin \phi \cdot \mathcal{I}m\{F_1 \tilde{\mathcal{H}} + x_B(F_1 + F_2)(\tilde{\mathcal{H}} + x_B/2\mathcal{E}) - x_B k F_2 \tilde{\mathcal{E}} \dots\}d\phi$$

Polarized beam, longitudinal target (BITSA)

$$d\sigma_{LL} = (A + B \cos \phi) \cdot \mathcal{R}e\{F_1 \tilde{\mathcal{H}} + x_B(F_1 + F_2)(\tilde{\mathcal{H}} + x_B/2\mathcal{E}) \dots\}d\phi$$

Unpolarized beam, transverse target (tTSA)

$$d\sigma_{UT} = \cos \phi \cdot \mathcal{I}m\{k(F_2 \mathcal{H} - F_1 \mathcal{E}) + \dots\}d\phi$$

Summary

- Elastic form factors provide a spatial imaging of charge and magnetization inside proton and neutrons in the transverse plane
- DIS and parton distribution functions provide a 1D imaging of the longitudinal momentum of partons inside nucleons
- GPDs provide a combination of both, and allow a 2+1D imaging of quarks (and gluons) in the transverse plane as a function of their longitudinal momentum.
- GPDs can be accessed experimentally through DVCS (lecture 2), but also through electroproduction of mesons at high momentum transfer Q^2 (lecture 3).